AlN/GaN/AlN HEMTs on Bulk AlN Substrates with High Drain Current Density > 2.8 A/mm and Average Breakdown Field > 2 MV/cm

Eungkyun Kim[1], Yu-Hsin Chen[2], Jimy Encomendero[1], Debdeep Jena[1,2], and Huili Grace Xing[1,2]
[1]*School of Electrical and Computer Engineering, Cornell University, Ithaca, New York 14853, USA*
[2]*Department of Materials Science and Engineering, Cornell University, Ithaca, New York 14853, USA*
Email: ek543@cornell.edu / Phone: (407) 409-4188

2024 Device Research Conference (DRC) | 979-8-3503-7373-8/24/$31.00 ©2024 IEEE | DOI: 10.1109/DRC61706.2024.10605544

Introduction: Wide energy bandgap and high saturation velocity of GaN have played a pivotal role in increasing the output power density (P_{out}) of a radio frequency (RF) transistor, allowing for an increased radar and communication system range. A further improvement in output power densities of GaN HEMTs is currently thermally limited due to the waste heat generated during the device operation in the channel layer. Therefore, to realize reliable and sustained operation at high P_{out}, thermal management in GaN HEMTs must be improved. We present AlN/GaN/AlN HEMTs, where an AlN buffer layer is homoepitaxially grown on bulk AlN substrates. In this heterostructure, AlN simultaneously offers an ultra-wide energy bandgap (~6.1 eV) and high thermal conductivity (340 W/m·K) [1]; the thermal advantage of an AlN buffer layer in HEMTs grown on SiC substrates has been recently confirmed by Soctera [2]. AlN homoepitaxy employed in our heterostructure further improves the thermal performance by potentially eliminating the thermal boundary resistance at the growth interface [3]. To this end, we report the on-current and breakdown behavior of HEMTs grown on Al-polar bulk AlN for the first time after the dramatically improved AlN homoepitaxy by MBE [4].

Experiments: The AlN/GaN/AlN heterostructure was grown by plasma-assisted molecular beam epitaxy (MBE) on free standing AlN substrates with a dislocation density < 10^4 cm^{-2} from Asahi Kasei Corporation [5]. The growth started with the in-situ cleaning of the AlN substrate using the Al-assisted surface cleaning technique [4], and the final as-grown epitaxial structure consists of a 2 nm GaN capping layer, a 3 nm AlN barrier, a 250 nm GaN channel layer, and a 500 nm AlN buffer layer. Device fabrication used a realigned gate-last process, beginning with an 80 nm n^+ GaN regrowth in the MBE chamber, followed by mesa isolation through BCl_3 inductively coupled plasma etch. Source and drain contacts were metallized by e-beam evaporation of Ti/Au. A rectangular gate was then defined by I-line photolithography for devices with a source-to-drain distance L_{SD} > 1 µm and a T-gate was defined by electron beam lithography for sub-micron devices. The final device structure along with an energy band diagram is shown in Fig. 1.

Results and discussion: Following the MBE growth, Hall-effect measurements were performed at room temperature using soldered corner indium contacts to the 2-dimensional electron gas (2DEG), revealing an electron mobility of 1080 $cm^2/V{\cdot}s$, a 2DEG density of 2.32×10^{13} cm^{-2}, and a corresponding sheet resistance of 250 Ω/sq. After the device fabrication, capacitance-voltage (C-V) measurements were performed using the gate and source contact of a HEMT as an anode and cathode, respectively. At equilibrium, a 2DEG density extracted from the C-V curve is 2.36×10^{13} cm^{-2}, as shown in Fig. 2, which aligns with the Hall-effect measurement result. DC transfer measurements performed on a device with L_{SD} = 3 µm and a gate length L_G = 0.8 µm (Fig. 3) revealed excellent gate control with a peak extrinsic transconductance g_m = 0.42 S/mm and a threshold voltage V_{th} ~ -2 V. Fig. 4 shows the three-terminal output characteristics. A peak drain current density $I_{D,max}$ = 1.6 A/mm with low output conductance (g_{ds}) was measured. Upon lateral scaling, $I_{D,max}$ increased to 2.85 A/mm while maintaining low g_{ds}. Next, pulsed I-V characteristics were measured with a pulse width of 500 nm with a 0.05% duty cycle to investigate dispersion control. As shown in Fig. 5, the AlN HEMT without a surface passivation layer showed minimal current collapse up to quiescent gate and drain bias of -6 V and 20 V. Dispersion control is expected to improve further upon surface passivation. Lastly, devices with different channel lengths were examined for breakdown to explore the potential for RF power amplification. Breakdown voltage was measured by increasing V_{DS} until catastrophic breakdown occurred with the gate voltage set below the threshold voltage. As illustrated in Fig. 6, sub-micron channel length devices with a T-gate exhibited an average breakdown field (E_{avg}) exceeding 2 MV/cm without a field plate, the highest E_{avg} and V_{BR} being 2.1 MV/cm and 137 V, respectively, for L_{GD} = 0.65 µm. Long channel devices with a rectangular gate showed a slightly lower E_{avg}, possibly caused by premature breakdown due to a higher gate leakage (causes are still under investigation). The off-state gate leakage current for T-gated devices (L_G = 0.1 µm) was ~ 5×10^{-6} A/mm whereas it was ~ 1×10^{-4} A/mm for rectangular-gated devices (L_G = 0.8 µm).

Acknowledgement: This work was supported in part by DARPA and SRC, and performed in part at the Cornell NanoScale Facility (an NNCI member supported by NSF Grant NNCI-2025233).

[1] R. Rounds *et al*., *Applied Physics Express* 11, 071001 (2018). [2] "Soctera improves GaN HEMT thermal performance." Semiconductor Today. https://www.semiconductor-today.com/news_items/2024/feb/soctera-090224.shtml (accessed Feb. 9, 2024). [3] G. Alvarez-Escalante *et al*., *APL Materials* 10, 011115 (2022) [4] Y. Cho *et al*., *Appl. Phys. Lett.* 116, 172106 (2020) [5] Z. Zhang *et al.*, *Appl. Phys. Lett.* 12, 124003 (2019)

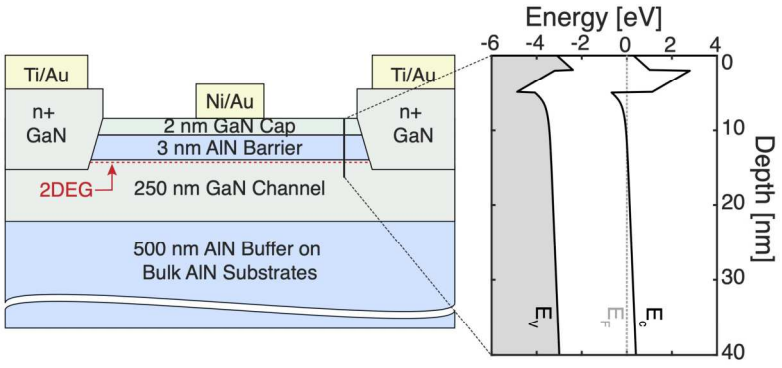

Fig. 1 Cross-sectional representation of a fully processed AlN/GaN/AlN HEMT and a simulated energy band diagram under the gate.

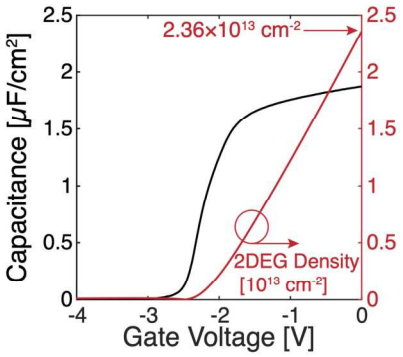

Fig. 2 C-V characteristics (black) of a HEMT and an extracted 2DEG density (red).

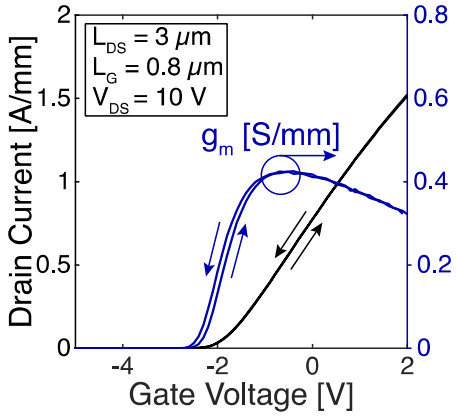

Fig. 3 Transfer characteristics of a HEMT showing peak extrinsic transconductance of 0.42 S/mm and a threshold voltage of -2 V.

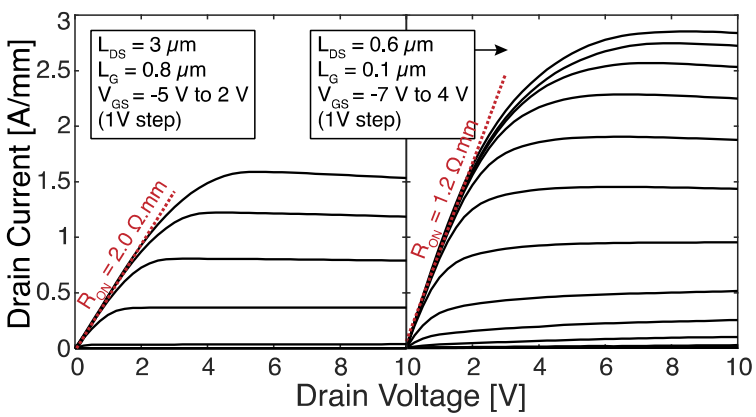

Fig. 4 Output characteristics of a long channel HEMT with a rectangular gate (left) and a scaled HEMT with a T-gate, showing a maximum drain current density of 1.6 A/mm and 2.85 A/mm, respectively.

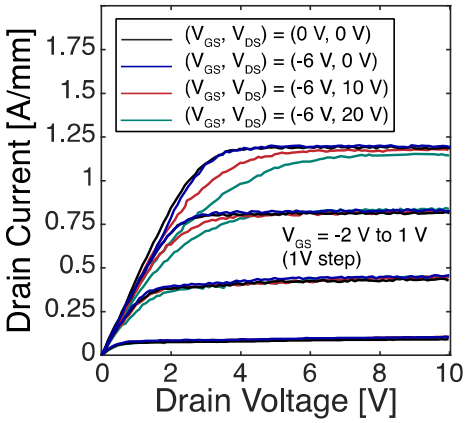

Fig. 5 Pulsed I-V characteristics of a HEMT without surface passivation at a gate bias of -2, -1, 0, and 1 V.

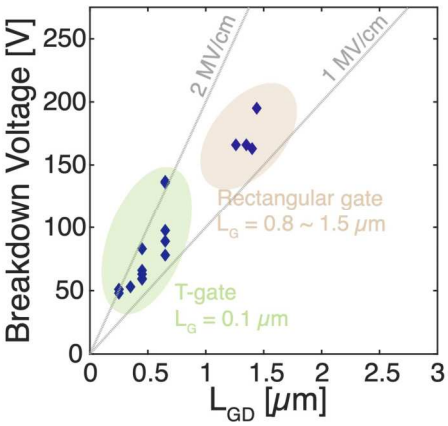

Fig. 6 Breakdown voltage of HEMTs as a function of a gate-to-drain distance.